

Received December 8, 2021, accepted December 19, 2021, date of publication December 23, 2021, date of current version January 4, 2022.

Digital Object Identifier 10.1109/ACCESS.2021.3137983

SatSysSim: A Novel Event-Driven Simulation Framework for DVB/RCS2 Performance Characterization

RENATO F. IIDA¹, PEDRO H. A. TRINDADE², BRUNO FARIA³, LEONARDO AGUAYO², AND ALEXANDER M. WYGLINSKI¹, (Member, IEEE)

¹Department of Electrical and Computer Engineering, WPI, Worcester, MA 01609, USA

²Electrical Engineering Department, Universidade de Brasília, Brasília 70910-900, Brazil

³Ektrum Tecnologia, Brasília 70701-000, Brazil

Corresponding author: Renato F. Iida (rfiida@wpi.edu)

This work was supported in part by the Coordenação de Aperfeiçoamento de Pessoal de Nível Superior (CAPES, Coordination for the Improvement of Higher Education Personnel) of the Brazilian Government.

ABSTRACT Satellite networks are expected to perform a vital role in future communication systems, with complex features and seamless integration with ground-based infrastructure. This paper presents a novel simulation framework capable of providing a detailed assessment of a satellite communication's network performance in realistic scenarios. The proposed framework employs an event-driven methodology, models the communications network as a DES (discrete event system), and focuses on the return link of the DVB-RCS2 standard. Three different scenarios demonstrate possible uses of the simulator's outputs to understand the network's dynamic behavior and achieve optimal system operation. Each scenario explores different features of the simulator covering a large territory with thousands of users, which in our case study was the country of Brazil.

INDEX TERMS DVB-RCS2, event-driven simulator, network performance, radio resource management, SymPy, system-level simulation, user allocation.

I. INTRODUCTION

The current percentage of the worldwide population with Internet access is nearly 60%, which is unequally distributed between developed and undeveloped countries. According to ITU-D statistics [1], the global availability of Internet access in 2019 per 100 users varied from 90% for developed countries to 20% for nations on the UN list of Least Developed Countries (LDCs), where poor social and economic development are the primary factors that limit ubiquitous and affordable Internet. In several countries, large territorial extension and geographic obstructions, such as mountains or dense forests, prevent the deployment of conventional cellular or cabled-based infrastructure.

Beyond the necessity to provide sufficient Internet access to the population, the recent increase in Machine-to-Machine (M2M) traffic, resulting from 5G/6G and IoT networks, imposes new challenges for service providers. Current

estimates predict that the number of devices connected to the Internet within five years will be approximately 25 billion [2], which further emphasizes the urgency for efficient utilization of radio resources and its integration among different Radio Access Technologies. This scenario is a challenging environment for network deployment and operation, not only in terms of Capital Expenditure (CAPEX) and Operating Expenses (OPEX) management, but also in the realms of initial network planning, heterogeneous traffic demand management, and coexistence with legacy infrastructure.

As an alternative telecommunications technology that can potentially serve inaccessible regions of the world, satellites can provide extended coverage for terrestrial networks and perform traffic offloading. Access to satellite communications can operate independently of ground-based cellular infrastructure, but the convergence trend to an IP-based service platform requires new approaches for combined planning and the operation of ground and space segments. Although challenges associated with the integration of cellular and satellite networks can be traced back to 2G GSM

The associate editor coordinating the review of this manuscript and approving it for publication was Ding Xu¹.

systems [3], recent studies [4] address new interoperability challenges and joint radio resource management (RRM) strategies for 5G and 6G network architectures.

For complex communication systems, the accurate inference of a network's performance requires system-level simulations, typically due to the difficulty of obtaining analytical solutions that consider all details related to protocol specifications and user behavior. Furthermore, the effect of complex relationships among the system's configuration parameters and the corresponding network operations can be better understood through a careful design of simulation scenarios. A controlled environment may stress the relevance of specific parameters that: (i) are not directly accessible by the network management system, or (ii) are out of the scope of a control system operated by the service provider. Planning and operations activities may use system-level simulations as a tool for potential savings on CAPEX and OPEX. Finally, representatives in standardization forums often use system-level simulations to address open issues, improve recommendations, and propose new features for the network nodes.

Considering the general scope of wireless networks simulation, reference [5] describes challenges for simulating 5G networks. In the context of Wireless Sensor Networks (WSNs), a review of simulation tools can be found in [6] and its references. Regarding the simulation of satellite communications [7] [8], describes modeling aspects for the medium access control (MAC) layer. More recently, NS-3 was used as the base framework engine to build a detailed implementation of RCS2 as described in [9] [10].

With a focus on the optimization of radio resources in DVB-RCS2, reference [11] presents an algorithm for the DVB-RCS2 superframe design and user allocation based on Jain's fairness index, but it does not explicitly mention the system performance in terms of capacity. In [12], the authors consider MF-TDMA allocation in a multi-spot scenario for Very High Throughput Satellites, but do not provide any details related to the MAC layer being employed as the logon phase and using random access channels.

A MAC procedure using Successive Interference Cancellation (SIC) with direct application to the MF-TDMA structure of RCS2 (CRDSA) can be found in [13]. An algorithm [14] created to optimize RCS2 radio resources; in this work, simulations were performed with fewer terminals and within a spatial range of 250 km.

In general, an event-driven simulation framework can be implemented in different ways and programming languages. The SimEvents framework [15] uses the Simulink and Matlab, and has been used in connected vehicle communications [16]. The framework presented in this paper employs a fusion of a static simulation used in standardization contributions [17] and the event-driven library SimPy [18].

There are other satellite simulators available in the open literature as well as commercially available software. A comparison of similar computer simulators to the proposed implementation is shown in Table 1. The decision to implement

the proposed simulator instead of using existing solutions were based on the following criteria as well as summarized in Table 1:

- **Easy to maintain:** The code base for the proposed implementation is version controlled and extensively tested using standardized approaches to assess simulator behavior.
- **Integration with link level from [22]:** There exists two other simulator platforms related to the proposed SatSysSim framework. One is a link level simulator and the other is antenna simulator, both of which were developed by a teams with regular meetings during the development of this framework. The system level simulator were created to provide an easy integration with those other two projects.
- **Join results with Anatel (Brazilian Government):** The proposed code base framework possesses results employing Anatel contributions related to satellite communications. Sharc [27] possesses several joint contributions with Anatel that have been proposed in ITU meetings such as [23] and [24]. This is important since the primary focus is the Brazil operating environment, and thus needs to consider the scope of the sponsors for this research project.
- **Compatible with DVB-RCS2:** The evaluation scenario for this proposed framework is targeting the Brazilian operating environment.
- **Control of the source code:** Due to the incorporation of sponsor intellectual property, the initial version of the proposed simulator is close source.
- **Extended from:** DVB-RCS2 simulators were created extending the functionality of previous simulators. This item show which software each framework used.

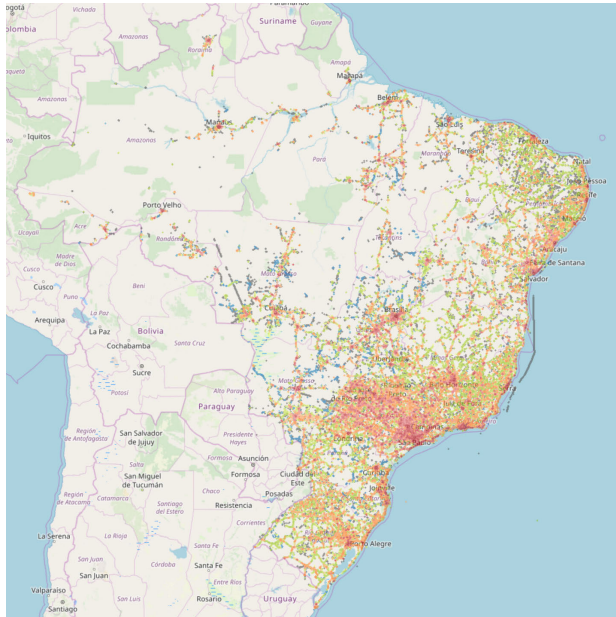
To our best knowledge, there is no similar published study with results obtained by system-level simulations considering an M2M traffic configuration. This paper proposes an event-drive framework for the system-level simulation of the resource allocation in DVB-RCS2 satellite networks. The contributions of this work consist of the following items:

- Application of the proposed event-driven simulation in large scale DVB-RCS2 deployments based on the structure shown in Figure 4.
- Incorporation of collision detection within the proposed framework and user customization covering different operation scenarios as shown in Figure 3.
- Implementation of a flexible platform for the evaluation and comparison of allocation algorithms inside a discrete event simulator as described in Section V-A.
- Creation of geospacial performance results to extend the analysis of the satellite network running using the proposed framework.

The rest of the paper is organized as follows: Section II describes the event driver used concepts to create the framework. Section III provides a brief description of the architecture of the DVB-RCS2 system. Section IV explains the

TABLE 1. Simulations frameworks features.

Features	SNS33 [19] [10]	DVB-S2/RCS simulator [20] [21]	Proposed Framework(SatSysSim)
Easy to maintain	Yes	Yes	Yes
Integration with link level from [22]	No	No	Yes
Join Results with Anatel (Brazilian Government)	No	No	Validation in [23] [24]
Compatible with DVB-RCS2	Yes	Yes	Yes
Control over the source code	Open source	Open source	Close source
Extended from	ns-3 [25]	OMNeT++ [26]	Sharc [27]

**FIGURE 1.** Typical cellular coverage in Brazil. Users are mainly located along the coastline and in the southeast region of the nation (adapted from [28]).

design, life cycle, and algorithms used in the proposed framework for the simulation of the DVB-RCS2. Section V illustrates the usage of the framework in three different scenarios. Section VI concludes with final comments and future steps in the framework development.

II. FUNDAMENTALS OF EVENT DRIVEN SIMULATION

As described in [30], input components interact inside a system to produce an output. The challenge is to create a model of a system that will provide a simulation in order to obtain an output based on these inputs. A Discrete Event System (DES) can be used to help model this unknown system. A DES implementation has a set of discrete states with an event-driven transition mechanism that triggers a state change to produce an output. If the original system to be modeled possesses a continuous-state behavior, its states smoothly change as time moves forward. However, when the original system is mapped to a DES implementation, only instantaneous transitions at predefined points in time need to be tracked. In this way, the simulation structure for an event-driven design requires a central scheduler to act as a bookkeeper and register all the event transition times in the model. As the events are asynchronous and may be concurrent, the register with the central scheduler must announce

any changes within the set of states. Furthermore, other events can be affected by the state changes, so a list of scheduled events to be processed at any simulation step must be kept.

For the DES implementation, the state space X is a countable set that of states s_i which is defined as:

$$X = \{s_1, s_2, \dots, s_n, s_{n+1}, \dots\}, \quad (1)$$

and a set of countable events E that consists of event e_i which is defined as:

$$E = \{e_1, e_2, \dots, e_k, e_{k+1}, \dots\}. \quad (2)$$

The time sequence of events to be processed is defined as a list L of pairs of events e_j and states s_i , which can be written as:

$$L = \{(e_1, t_1), (e_2, t_2), (e_3, t_3), \dots\}. \quad (3)$$

Furthermore, the simulation runs in a way such that there is a time ordered scheduled event list L_s , with the smallest schedule time processed first. This way, the first event in the list is always the triggering event that produces the changes in the X set.

The mapping of these events and states in this framework was performed using the SimPy library [18], which implements event-driven behavior using the Python programming language. As Python allows for object-oriented programming, it creates a generator for each event that can be mapped to a function or a class method. When an event is triggered, it awakens other events registered in a core class called `environment`. This way, e_1 is mapped to a function that also defines the corresponding waking time t_1 . Details of the implementation require that, in order to register, events share the same `environment`. This object also controls time sequencing.

III. SYSTEM ARCHITECTURE

Before the details of the simulator's design and its capabilities are provided, a brief architectural description of the DVB-RCS2 standard [31] is provided below. RCS2 makes use of a hierarchical and flexible frame structure. The minimum resource block that composes the frame is called the bandwidth-time unit (BTU), which has a configurable length (in symbols) and symbol rate.

A timeslot (TS) is a contiguous sequence of BTUs in time. A TS may possess a different size based on the number of BTUs assigned to it. Furthermore, a TS is the minimum allocation unit used by the packet scheduler. Users with different throughput requirements may be allocated to TSs of

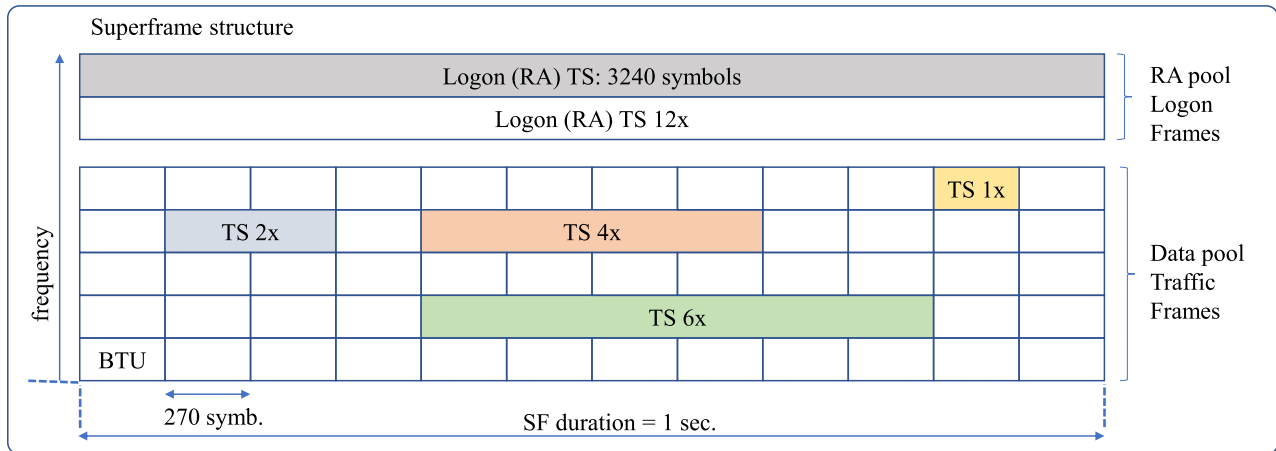


FIGURE 2. Organization of the MF-TDMA hierarchy in the simulator (SF, frame, TS and BTU) with two pools of channels: RA for signaling and DA for traffic data. All logon messages use 12 BTUs as a worst case for Waveform 41 in Table 10.4 in [29]. The data BTUs are dynamically allocated, based on current E_s/N_0 and recommended waveforms, both obtained from link level simulations.

different lengths, which allows the allocation algorithm to manage radio resources. All lengths allowed by the RCS2 physical layer standard [32], which also called burst lengths, are defined by the amount of data symbols assigned to a set of distinct Adaptive Modulation and Coding Schemes (ACMs).

A third element of hierarchy is the frame, which is a set of TSs arranged in both time and frequency. It is incorporated into a superframe (SF), which is an arrangement of frames that is ordered both in time and frequency. A superframe sequence (SFS) is an ordered time sequence of superframes. An RCS2 system may use different SFSs within a satellite transponder according to the overall bandwidth requirements or capacity restrictions. From an allocation algorithm perspective, a user is a TS number identified by its position inside a particular frame within an SF. The global configuration is communicated to all MCTs by tables (SCT/FCT2/BCT/TBTP2) that are broadcast to all users via a signaling procedure. Details can be found in [32] and [29].

Figure 2 illustrates a simplified view of the MF-TDMA, which is employed within the proposed simulator. The RA (Random Access) pool consists of logon frames represented by incoming RCST (Return Channel via Satellite Terminal) login requests. The Deterministic Access (DA) pool corresponds to the RCST data traffic frames. Inside a DA pool, the packet scheduler is active and performs the TS allocation procedure defined by the algorithms described in Section V. The burst lengths are 266, 536, 1616, and 3236 symbols, respectively. Adding four symbols as guard symbols results in TS lengths of 270, 540, 1620, and 3240 symbols, all multiples of 270 ($1\times$, $2\times$, $6\times$, and $12\times$). The largest one ($12\times$) is also selected to carry random access (RA) signaling, as the standard assigns it to the most robust ACMs.

DVB-RCS2 standards also define four different types of mechanisms to assign resources to RCSTs: Constant Rate Assignment (CRA), Free capacity Assignment (FCA), Rate-Based Dynamic Capacity (RBDC), and Volume-Based Dynamic Capacity (VBDC). In CRA, the data rate is

negotiated before channel assignment and guaranteed by the Service Level Agreement (SLA) between the client and the service provider. The FCA mechanism allocates spare resources that might not have been allocated after a Dynamic Bandwidth Allocation (DBA) process performed at the Network Control Centre (NCC). RBDC and VBDC use capacity requests— either a volume of data or data rate request— from the RCST, to define the optimal resource allocation distribution. This method is usually referred to as Bandwidth on Demand (BoD) or Demand Assigned Multiple Access (DAMA).

IV. PROPOSED FRAMEWORK

The proposed simulator framework is presented in Figure 4. Text files contain input parameters related to the link nodes (RCSTs, satellite, NCC), channel modeling, MF-TDMA hierarchy, link-level performance curves, traffic profiles, antennas, and simulation campaigns. The event handling block that corresponds to the discrete-event simulation is described later in this section. During the simulation, each new superframe generates partial results in the output files. After the simulation reaches the end, the output files are post-processed to generate the plots indexed by load or simulation time. The simulator also provides geo-referenced results for an analysis of bandwidth utilization. Some of those results are shown and discussed in Section V.

At the core of the simulator is a discrete event manager responsible for handling the dynamics of all connections in the network. SimPy was used as the discrete-event framework for the simulator implementation. For example, the SimPy framework handles multiple events related to the arrival and departure of RCSTs, their access to the network, and packet transmission. One important event is a possible packet collision in the RA pool during the logon procedure. In particular, SimPy provides a `store` object [33], which is a FIFO (first-in, first-out) storage object that can trigger other processes whenever its contents are changed. The MF-TDMA structure

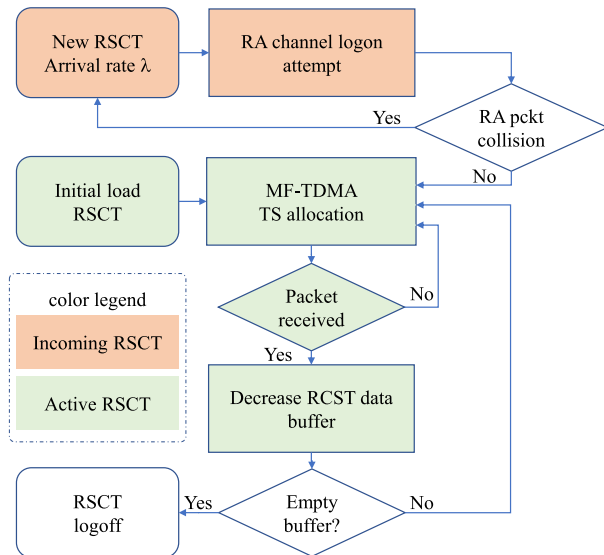


FIGURE 3. Terminal lifecycle in the system. Optimization of resources within the RCS-2 MF-TDMA structure is performed at each superframe.

follows the structure of Figure 2, where each channel in frequency is represented by one `store` object in memory. When a packet is inserted into the `store` object, which represents a packet being sent through the channel, the receiver process becomes awake (here modeling the NCC reception), handles the triggered event, and checks if more than one packet was received at the same time in order to detect collision.

Figure 3 shows the life cycle of each user (or RCST) in the network. There are two possible ways that an RCST can enter the system, and once accepted, becomes part of the *active users* set. The first way is when the RCST is part of the initial load, defined by the simulation scenario setup. In this case, the RCST is already an active user. The second follows a Poisson probability distribution with an arrival rate λ generated at the start of each new SF. The arriving RCST needs to follow a logon process, which includes an attempt to get a resource from the RA pool. After a successful login (without collision with other RCSTs), an algorithm performs the proper TS allocation of the RCST's data traffic at the DA pool.

Each active user allocated in a superframe has a data buffer to transmit. When an RCST transmits a packet, it is evaluated for packet error rates through a combination of a link budget procedure and a check of E_s/N_0 requirements for the waveform used for transmission. All E_s/N_0 curves are obtained from an external link-level simulator [22] that handles the details of the channel coding and digital modulation for all ACMs in the standard documentation [34]. It is worth noting that link-level results affect system-level performance. From the perspective of the system-level simulator operation, link-level curves are tables retrieved at the beginning of the simulation. If changes in the receiver design affect the performance, the corresponding new tables can be replaced without changing the rest of the code. Also, it is possible to use the

reference values for physical layer performance from [29, Sect. 10.2].

If a packet is successfully received, the total amount of data remaining in the RCST's buffer is decreased. If there is an error, the RCST retransmits the packet and maintains its active user status. When a new SF is created, the deterministic allocation algorithm handles the currently active RCSTs and all RCSTs that had their channel requests granted from the previous SF.

As the simulation continues to operate, output files with partial results are produced. A set of key performance indicators (KPIs) were selected in this simulation framework to assist with the system performance analysis, such as latency due to the logon process, the number of frequencies used in the SF, the raw throughput at the PHY layer, and the goodput at the MAC layer. Results are collected for each RCST and for all SFs in the simulation. This allows for the post-processing and statistical analysis of the performance indicators.

A. RESOURCE ALLOCATION ALGORITHMS

To assess the resource allocation functionality in the event-driven system-level simulation software, we implemented simple versions of the CRA and FCA mechanisms.

For the CRA mechanism, we chose an algorithm based on a greedy strategy, referred to in this work as the Greedy Priority Allocation (GPA). It is defined in Algorithm 1. It traverses the SF DA pool sequentially, allocating at each step the necessary timeslot length to meet the RCST's QoS requirements. The allocation continues until the exhaustion of SF resources. Supposing an agreed data rate R_i to the RCST i and defining $T_{SF} = 1$ second, the necessary timeslot length L_i (in BTUs) can be calculated as:

$$L_i = \left\lceil \frac{R_i}{P_i} \right\rceil B_i, \quad (4)$$

where P_i is the payload in the ACM of the RCST, which is a function of its E_s/N_0 in the return link connection. B_i is the value of BTUs per burst, which is also referred to as the BTUs per waveform. A set of $k = 4$ dynamic resource allocation (DRA) blocks, which corresponds to the four TS lengths ($1 \times$, $2 \times$, $6 \times$ and $12 \times$) as described in Section III.

Algorithm 1 describes the procedure for the GPA algorithm. While there are BTUs available in a Superframe (SF BTUs) and a feasible DRA channel is available. GPA algorithm must inspect if allocating the current RCST i is feasible. In case of true condition, the RCST must be allocated, and the utilized BTUs must be subtracted from the total available. The final step is to attend to the next RCST in the queue. In case of false condition, GPA algorithm skip to the next DRA channel and reiterate.

The allocation procedure also prioritizes users according to their SNR. RCSTs with a larger SNR will be served first, in contrast to the RCSTs with lower SNR, which typically need a more significant portion of the SF in order to complete their QoS requirements.

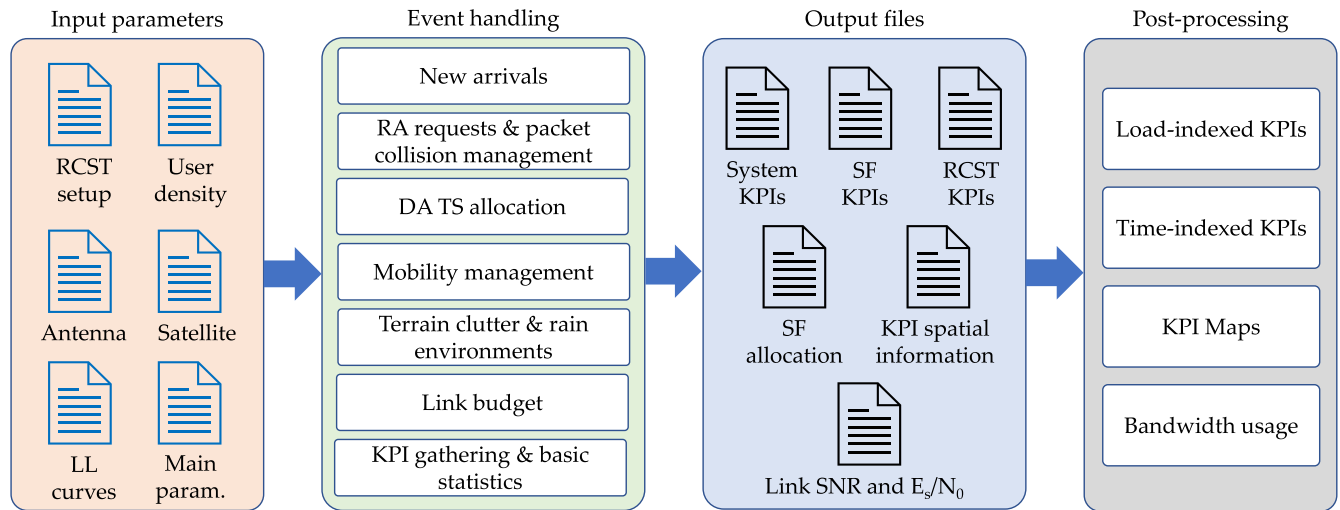


FIGURE 4. General structure of the system-level simulator, with examples of input and output files. The event handling subsystem is responsible for RCSTs transmission management.

Algorithm 1 GPA - Greedy Priority Allocation

```

1: Sort RCST queue based on SNR
2: while SF BTUs > 0 and DRA  $k \leq k_{\max}$  do
3:   if DRA  $k$  BTUs  $-L_i \geq 0$  then
4:     Allocate  $L_i$  to RCST  $i$ 
5:     Subtract  $L_i$  from DRA  $k$  BTUs and SF BTUs
6:     Go to next RCST  $i + 1$ 
7:   else
8:     Go to next DRA  $k + 1$ 
9:   end if
10: end while

```

To verify the simulator performance in an FCA allocation context, we employed an algorithm that equally divides the surplus capacity between each RCST. In this algorithm, called Simple Division Algorithm (SDA), which is presented in Algorithm 2, the scheduler equally divides the number of BTUs in an SF to each RCST. This strategy is not a greedy one, as it needs the information of all RCSTs in the queue to perform the resource allocation. If any of those RCSTs do not meet the QoS requirement, then the least element in the RCST list is temporarily discarded to be allocated in the next Superframe. This process repeats until all RCSTs meet their QoS requirements.

Algorithm 2 explains the SDA algorithm operation. The total number of BTUs in a SuperFrame (SF BTUs) is divided by the total number of RCSTs to be served (N). This variable is denoted as Div . It must be verified whether Div is greater than all RCSTs' required timeslots (TS_i), *i.e.* whether all RCSTs receive more BTUs than the minimum to satisfy the QoS requirements. If this is the case, Div as a multiple of the waveform length in BTUs must be allocated to each RCST. Otherwise, one less RCST should be served, and the algorithm should be reiterated until all RCSTs allocated satisfy the minimum QoS requirements.

Algorithm 2 SDA - Simple Division Allocation

```

1:  $Div = SF\ BTUs / N$ 
2: while any  $TS_i - Div < 0$  do
3:   Pop last RCST in the RCSTs list
4:   Decrement  $N$ 
5:    $Div = SF\ BTUs / N$ 
6: end while
7: Allocate to each RCST  $Div$  as a multiple of the waveform length in BTUs.

```

V. SIMULATION RESULTS

Through the use of the proposed simulation framework, which was designed to analyze and evaluate solutions for problems that appear when performing planning and scaling activities in satellite networks, proposed use cases are described below.

We implemented two different algorithms to assess multi-user scheduling and allocation within the RCS2 MF-TDMA structure to provide a comparative study. The optimal resource allocation problem for the reverse link multiple access is investigated thoroughly in the academic literature [35], [36] [12], although it is rarely analyzed through the entire DVB-S2X/DVB-RCS2 system pipeline, with a realistic link performance, request queues, and spatial distribution for the RCSTs. In this case, we addressed all of these within the constraints of the ETSI RCS2 standards [32], [37] [38], which implied a need for a detailed evaluation of link performance for each user in the spatial dimension. End-to-end link quality is affected by the channel conditions and satellite footprint, both of which are functions of space. Hence, the use of maps and location coordinates, which is particularly relevant to satellite communications, was considered in this study. The last problem that was addressed focused on the spectrum allocation decision; namely, the amount of frequency allocated for both login and traffic channels, and how this proportion would affect the global behavior of the network.

TABLE 2. Parameters used in the system-level simulations.

Parameter	Value	Unit
Simulation time	25	seconds
Superframe duration	1	second
Bandwidth per BTU	150	kHz
Minimum RCST data rate	10	kbits/s
RCST buffer size	10	kbytes
DA pool bandwidth	900	kHz
RA pool bandwidth	600	kHz

We considered values of mobile users' traffic demands from low to moderate data rates (below 100 kbits/s). The chosen geographical area was the entire country of Brazil, since it possesses the following features: (i) its geographical extension, suited to be covered by the footprint of GEO satellites; (ii) its span of different climate zones, which include both rainy and dry regions; and (iii) the uneven spatial distribution of its population, which has a higher density in the littoral coast and the south/southeast areas. Figure 1 depicts a cellular coverage map of Brazil that verifies a concentration of available wireless services in the regions mentioned above.

Below, the features of the simulator are evaluated through an analysis of the satellite network behavior in three cases: (i) choice of the allocation algorithm, (ii) results displayed spatially over a geographical territory, and (iii) bandwidth requirements for RA and DA pools. Each simulation scenario was mainly defined by the initial RCSTs in the system and the arrival rate λ of new ones. Other system parameters with fixed values within the scope of this paper are presented in Table 2.

A. COMPARISON OF RESOURCE ALLOCATION ALGORITHMS

The first application example that was chosen to show the features of the system level simulator was to evaluate the impact of using distinct user allocation algorithms and verify how those strategies influence the overall network performance. We implemented the GPA and SDA algorithms to evaluate how the simulator can predict network behavior in a realistic scenario.

Each load point $N_{U,t}$ in the network represents the number of RCSTs in the system. In a simulation, $N_{U,t}$ is defined by:

$$N_{U,t} = N_{U,0} + \lambda T_{sim}, \tag{5}$$

where $N_{U,0}$ is the initial number of users, λ is the arrival rate, and T_{sim} is the value of simulation time taken from Table 2. Here we addressed the effect of changing $N_{U,0}$ and λ of new users according to Table 3. For both options of the allocation algorithms, and for different loads, Figure 5 shows that the total throughput was similar in an SF regardless of the allocation algorithm.

However, it is possible to verify from Figure 6 a difference between GPA and SDA when the average throughput per RCST is considered. While the GPA algorithm attempted to maintain a GBR of 10 kbits/s for each user, the SDA algorithm used spare BTUs to increase individual data rates. On the other hand, as the load increased, unused resources in

TABLE 3. Load points for simulation scenarios.

Parameter	Initial value	Step	Final value
$N_{U,0}$	100	100	400
λ	10	20	70

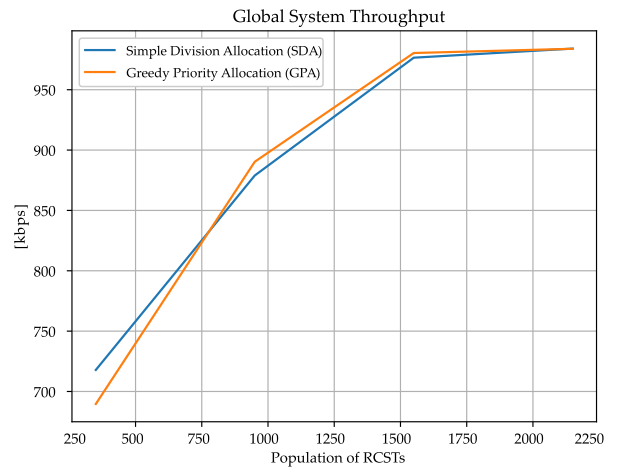


FIGURE 5. Global throughput of GPA and SDA allocation algorithms for different load points.

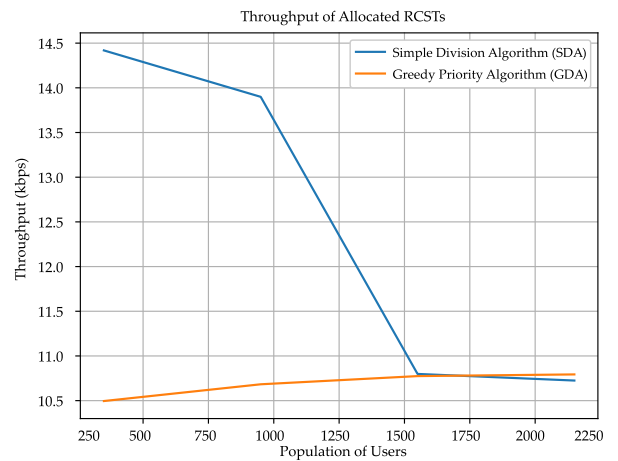


FIGURE 6. Average throughput per user of each allocation algorithm for different load points.

an SF gradually disappeared, and the SDA algorithm could not make use of them.

There was also a second impact on the network performance if the dynamic behavior of active RCSTs in the system is considered. As each RCST had a buffer with data to transmit, there were differences in the time needed to empty them. As shown in Figure 7, this time duration was shorter when using the SDA algorithm when compared to the GPA algorithm. As a global result, there was a better dynamic utilization of the DA pool.

Another way of interpreting this result is by observing Figure 8. In this case, simulations showed that the average number of active users in an SF was different for both cases. With the GPA algorithm, there were more users when compared to the SDA algorithm, but they remained in the system for a longer time. This result reinforces the need for a policy

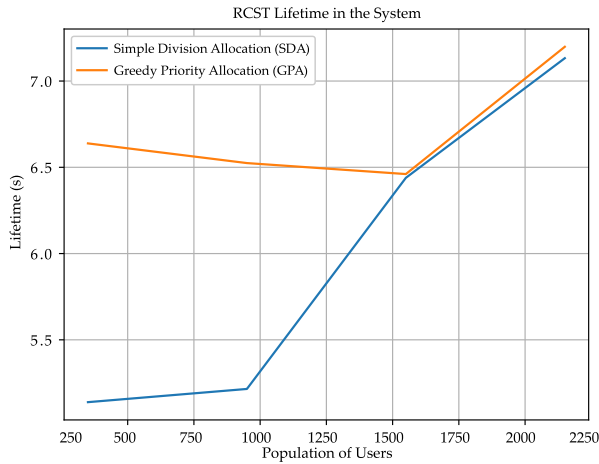


FIGURE 7. Average lifetime in seconds of completed users of each allocation algorithm for each load point.

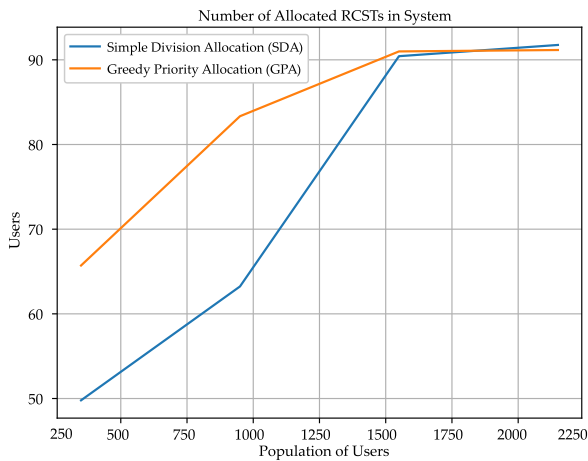


FIGURE 8. Behavior of the mean number of simultaneous active users for different load points.

of load management that uses the flexibility of dynamical allocation of the RCS2 standard and the admission policy of new users. Finally, while the GPA algorithm allows for a distribution that will always satisfy the predefined rate requirements, it may also waste bandwidth capacity as it only allocates the necessary amount of BTUs to each RCST. This effect was most evident in scenarios with low values of the rate of arrivals λ .

B. GEOSPATIAL NETWORK PERFORMANCE RESULTS

Beyond the statistics obtained from the MF-TDMA structure, the simulator displayed spatial results. The simulator produced the geographical information by calculating the link budget for each point on the map. The complete calculation required information about the transmitter, receiver, channel impairments, and noise, such as transmitted power; the position of the satellite (which in this case was geostationary); the channel modeling (free path loss and troposphere effects); and the main characteristics of the antennas used on link endpoints (NCC and RCSTs), namely the antenna gains G and their effective noise temperature T . For the satellite antenna,

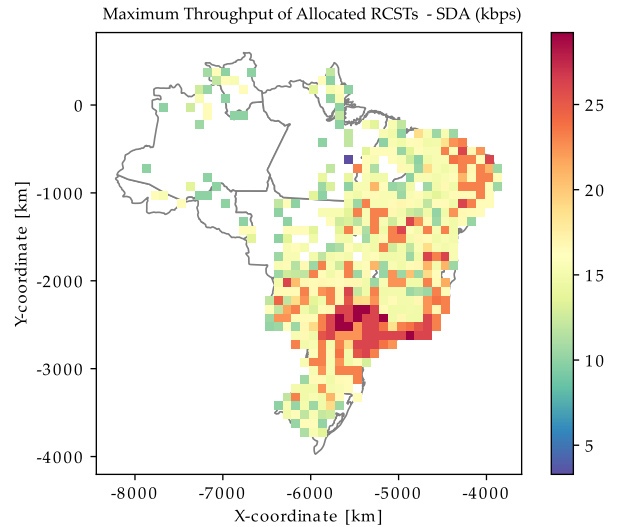


FIGURE 9. Heat map of maximum RCST data throughput under the selected coverage area using the SDA algorithm.

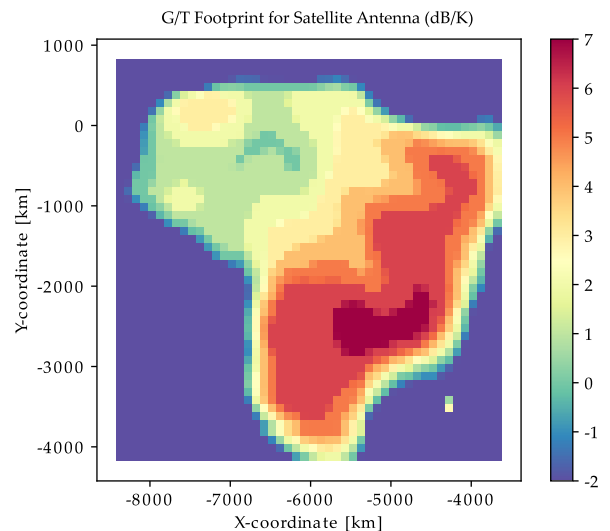


FIGURE 10. Heat map of G/T for a GEO satellite, used as a parameter to obtain spatial information of system performance.

it was also possible to use the G/T footprint for the coverage area, as G and T were not always separately available.

One example is shown in Figure 9, which shows the maximum throughput achieved by one user born in the system at specific latitude and longitude coordinates. The start location of the RCST was generated using a probability density function that considers the population density in the region of interest. It is possible to verify that the SDA algorithm provided maximum throughput in regions with higher G/T by following the G/T footprint depicted in Figure 10. As shown by the results of the link budget procedure, areas with better performance corresponded to regions with larger values of E_s/N_0 .

C. EVALUATION OF RANDOM ACCESS AND DATA CHANNEL BANDWIDTHS

According to the life cycle diagram in Figure 3, every RCST that attempted to enter the system needed to request an

TABLE 4. Scenarios for analysis of bandwidth allocated to RA and DA resource pools.

Scenario	BW RA (kHz)	BW Data (kHz)
A	150	1350
B	300	1200
C	450	1050

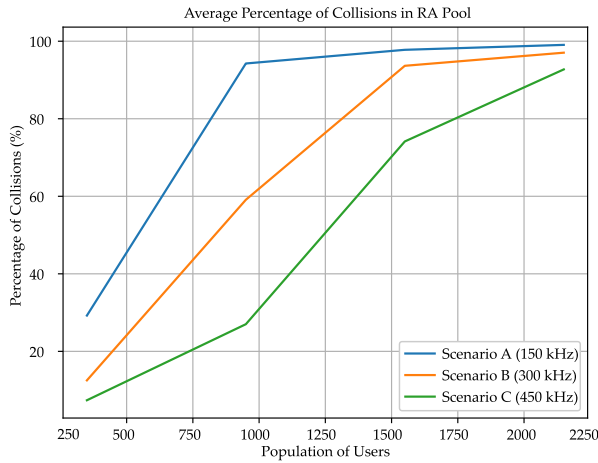


FIGURE 11. Average percentage of collisions in the RA frames for different proportions of RA and DA pools. In all cases, the system has the same total bandwidth.

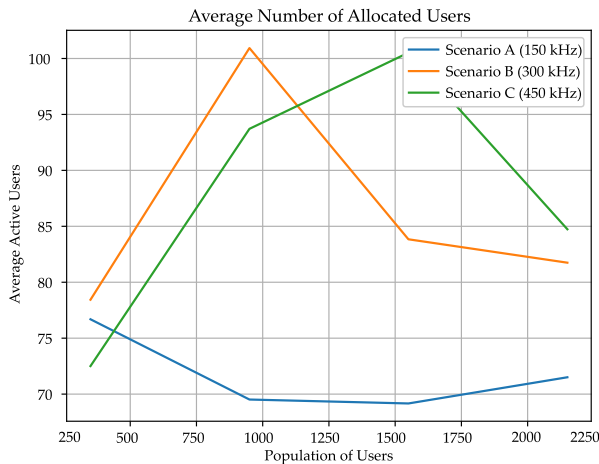


FIGURE 12. Average number of active users in the system affected by the collision rates shown in Figure 11.

access channel (RA). It was of practical interest to set the best proportion of both pools, RA and DA, to maximize the overall system spectral efficiency. We fixed the total system bandwidth for the comparisons performed here, but the bandwidth values assigned to RA and DA pools were different, as depicted in Table 4.

In order for the results from Figures 11, 12, and 13 to be understood, they must be analyzed together. Considering the values of Table 4, Scenario A had the lowest level of resources assigned to the RA pool; as a result, it had the highest collision rate at every load point, as shown in Figure 11. When the system had more collisions, it increased the queue of users attempting to enter the system, and fewer users entered as

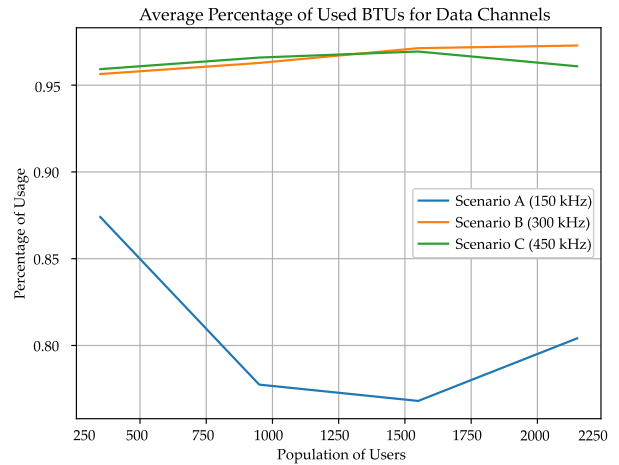


FIGURE 13. Average percentage of BTU usage for different proportions of RA and DA pools using the same scenarios as Figures 11 and 12.

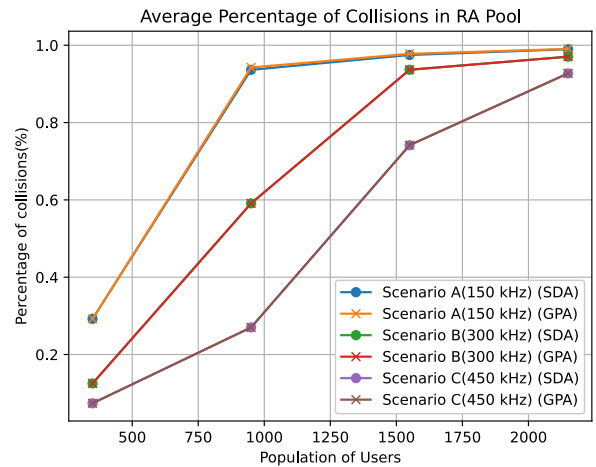


FIGURE 14. Average percentage of collisions in the RA frames for 3 scenarios described in table 4 with both allocation strategies. SDA uses circle markers and GPA uses X markers.

allocated users. The consequence of the high collision rate, as shown in Figure 12, was that system A had the lowest number of active users at any load point, despite having a higher number of channels to be used in allocation. Thus, theoretically, Scenario A could handle more users, but those users never entered the system because of the collision in the request to transmit. Scenario B started to decrease at a user load point of 1500 for the same reason because the collision rate was above 90%. Scenario C reached this decrease at 2000 users for the same reason. Therefore, the number of BTU in random access area needs to be optimized by the arrival rate of the new users in order to avoid this high collision rate. The expected behavior of the system without the high collision rate is shown in Figure 8.

Figure 13 shows how Scenario A could handle more users if more users had been allowed to enter the system, as more than 10% of the BTU resources were unused. This could have been related to the allocation algorithm, but that was not the case in this scenario. There were fewer users of user in this system because those users could never be allocated in the

system, due to the collision rate always being above 80% after the 750 load point. The behavior of the random access pool are not affected by the SDA and GPA allocation as shown in Figure 14 because the curves of allocation overlap within the same scenario. The reason is the collisions happen during the random access phase and it happens before the RCSTs become active and enter in the green area of the life cycle depicted in Figure 3.

VI. CONCLUSION

This paper presented an event-driven, system-level simulator with implementation details for the PHY and MAC layers compliant to the DVB-RCS2 ETSI standard. We provided three use case examples for the proposed simulation framework in order to help evaluate and design a GEO satellite system with a large coverage area within a realistic scenario. This proposed framework showed two allocation strategies, and can be used in the future to test and evaluate new allocation strategies. Additionally, the output was georeferenced and plotted on the map of the scenario. Finally, the collision detection mechanism showed how this could affect the performance of the whole system. The framework is also capable of providing an extensive set of results and KPIs, such as packet loss rate (PLR). Performance of other receivers will be presented in future works and an extension of the code to handle LEO trajectories is currently under development. The purpose of this article is the focus on the behaviour and analysis of DVB-RCS2. Optimization of the code is a topic of future research, as well as an evaluation of the performance and code complexity.

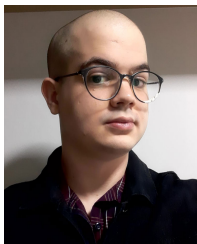
REFERENCES

- [1] ITU-D. *ITU Telecommunication Development Sector Statistics*. Accessed: Dec. 23, 2021. [Online]. Available: <https://www.itu.int/en/ITU-D/Statistics/Pages/stat/default.aspx>
- [2] Ericsson Mobility Report. *IoT Connections Outlook*. Accessed: Jun. 1, 2020. [Online]. Available: <https://www.ericsson.com/en/mobility-report/reports/june-2020/iot-connections-outlook>
- [3] *GEO-Mobile Radio Interface Specifications (Release 3): Third Generation Satellite Packet Radio Service: Part 1: General Specifications; Sub-Part 3: General System Description*, document GMR-13G41.202-TS 101 376-1-3 V3.1.1 (2009-07), ETSI, 2009.
- [4] P. Wang, J. Zhang, X. Zhang, Z. Yan, B. G. Evans, and W. Wang, "Convergence of satellite and terrestrial networks: A comprehensive survey," *IEEE Access*, vol. 8, pp. 5550–5588, 2020.
- [5] Y. Wang, J. Xu, and L. Jiang, "Challenges of system-level simulations and performance evaluation for 5G wireless networks," *IEEE Access*, vol. 2, pp. 1553–1561, 2014.
- [6] A. Nayyar and R. Singh, "A comprehensive review of simulation tools for wireless sensor networks (WSNs)," *J. Wireless Netw. Commun.*, vol. 5, no. 1, pp. 19–47, Jan. 2015.
- [7] D. P. Connors, B. Ryu, and S. Dao, "Modeling and simulation of broadband satellite networks. I. medium access control for QoS provisioning," *IEEE Commun. Mag.*, vol. 37, no. 3, pp. 72–79, Mar. 1999.
- [8] H. Al-Hraishawi, E. Lagunas, and S. Chatzinotas, "Traffic simulator for multibeam satellite communication systems," in *Proc. 10th Adv. Satell. Multimedia Syst. Conf. Commun. Workshop*, 2020, pp. 1–8.
- [9] J. Puttonen, S. Rantanen, F. Laakso, J. Kurjenniemi, K. Aho, and G. Acar, "Satellite model for network simulator 3," in *Proc. ICST*, Aug. 2014, pp. 86–91.
- [10] J. Puttonen, L. Sormunen, and J. Kurjenniemi, "Radio resource management in DVB-RCS2 satellite systems," in *Proc. 34th AIAA Int. Commun. Satell. Syst. Conf.*, Oct. 2016, pp. 18–20, 2016, doi: [10.2514/6.2016-5734](https://doi.org/10.2514/6.2016-5734).
- [11] D.-H. Jung, M.-S. Shin, and J.-G. Ryu, "Fairness-based superframe design and resource allocation for dynamic rate adaptation in DVB-RCS2 satellite systems," *IEEE Commun. Lett.*, vol. 23, no. 11, pp. 2046–2049, Nov. 2019.
- [12] J.-M.-R. Bejarano, C. Miguel Nieto, and F. J. Ruiz Pinar, "MF-TDMA scheduling algorithm for multi-spot beam satellite systems based on co-channel interference evaluation," *IEEE Access*, vol. 7, pp. 4391–4399, 2019.
- [13] E. Casini, R. D. Gaudenzi, and O. D. R. Herrero, "Contention resolution diversity slotted ALOHA (CRDSA): An enhanced random access scheme for satellite access packet networks," *IEEE Trans. Wireless Commun.*, vol. 6, no. 4, pp. 1408–1419, Apr. 2007.
- [14] A. Pietrabissa and A. Fiaschetti, "Dynamic uplink frame optimization with adaptive coding and modulation in DVB-RCS2 satellite networks," *Int. J. Satell. Commun. Netw.*, vol. 31, no. 3, pp. 123–139, May 2013.
- [15] W. Li, R. Mani, and P. J. Mosterman, "Extensible discrete-event simulation framework in simevents," in *Proc. Winter Simulation Conf. (WSC)*, 2016, pp. 943–954.
- [16] Y. Zhang, C. G. Cassandras, W. Li, and P. J. Mosterman, "A discrete-event and hybrid simulation framework based on simevents for intelligent transportation system analysis," *IFAC-Papers in line*, vol. 51, no. 7, pp. 323–328, 2018.
- [17] *Sharing Studies Between IMT-2020 and the Radio Astronomy Service in the 42.5-43.5 GHz Band*, document 319, ITU Working Draft Proposed Standard, 2018.
- [18] *Simpy Documentation*. Accessed: Dec. 23, 2021. [Online]. Available: <https://simpy.readthedocs.io/en/latest/>
- [19] J. Puttonen, S. Rantanen, F. Laakso, J. Kurjenniemi, K. Aho, and G. Acar, "Satellite model for network simulator 3," in *Proc. 7th Int. Conf. Simulation Tools Techn.*, 2014, pp. 86–91.
- [20] V. Boussemart and H. Brandt, "A tool for satellite communications advanced DVB-RCS/DVB-S2 system and protocol simulator," in *Proc. 10th Int. Workshop Signal Process. Space Commun.*, IEEE, 2008, pp. 1–5.
- [21] V. Boussemart and H. Brandt, "A system simulator for advanced DVB-S2/RCS multibeam systems," German Aerosp. Center, Germany, Tech. Rep., 2009. [Online]. Available: <https://elib.dlr.de/58749/1/dlrk.pdf>
- [22] R. A. R. Fischer and J. P. Leite, "DVB-RCS2 satellite standard performance assessment through a link-level Python simulator," in *Proc. 38th Brazilian Symp. Telecommun.*, Florianópolis, Brazil, Nov. 2020, pp. 1–2.
- [23] Anatel. (2018). *Sharing Studies Between IMT-2020 and the Radio Astronomy Service in the 42.5-43.5 GHz Band*. [Online]. Available: https://www.itu.int/md/R15-TG5.1-C-0319/_page.print
- [24] (2018). *On the Convergence of Monte-Carlo Approach for Sharing and Compatibility Studies Between IMT-2020 and Other Services*. [Online]. Available: <https://www.itu.int/md/R15-TG5.1.AR-C-0241/fr>
- [25] G. F. Riley and T. R. Henderson, "The NS-3 network simulator," in *Models Tools for Networking Simulation*, K. Wehrle, M. Günes, and J. Gross, Eds. Cham, Switzerland: Springer, 2010, pp. 15–34, doi: [10.1007/978-3-642-12331-3_2](https://doi.org/10.1007/978-3-642-12331-3_2).
- [26] A. Varga, "The OMNeT++ discrete event simulation system," in *Proc. Eur. Simulation Multiconf. (ESM)*, Prague, Czech Republic, Jun. 2001.
- [27] Anatel. (2018). *SHARC, Simulator for Use in SHARING and Compatibility Studies of Radiocommunication Systems*. [Online]. Available: <https://github.com/SIMULATOR-WG/SHARC>
- [28] Nperf. (May 2019). *Coverage Map*. [Online]. Available: <https://www.nperf.com/pt/map/BR/-/-/signal/?ll=-15.126554432601873&lg=-51.6%44999999999999&zoom=4>
- [29] *Digital Video Broadcasting (DVB): Second Generation DVB Interactive Satellite System (DVB-RCS2): Part 4: Guidelines for Implementation and Use of EN 301 545-2*, document TS 101 545-4 V1.1.1, ETSI, 2014.
- [30] C. G. Cassandras and S. Lafortune, *Introduction to Discrete Event System*. New York, NY, USA: Springer, 2008.
- [31] *Digital Video Broadcasting (DVB): Second Generation DVB Interactive Satellite System (DVB-RCS2): Part 1: Overview and System Level Specification*, ETSI, Sophia Antipolis, France, pp. 1–22, 2014.
- [32] *Digital Video Broadcasting (DVB): Second Generation DVB Interactive Satellite System (DVB-RCS2): Part 2: Lower Layers for Satellite standard*, document EN 301 545-2 V1.2.1, ETSI, 2014.
- [33] *Store Object Documentation*. Accessed: Jun. 1, 2020. [Online]. Available: https://simpy.readthedocs.io/en/latest/api_reference/simpy.resources.html#simpy.resources.store.Store
- [34] *Digital Video Broadcasting (DVB): Second Generation DVB Interactive Satellite System (DVB-RCS2): Part 2: Lower Layers for Satellite standard*, document EN 301 545-2-V1.2.1, ETSI, 2014, pp. 1–239.
- [35] G. Seco-Granados, A. Vazquez-Castro, A. Morell, and F. Vieira, "SAT03-6: Algorithm for fair bandwidth allocation with QoS constraints in DVB-S2/RCS," in *Proc. Globecom*, Jan. 2006, pp. 1–6.

- [36] A. Morell, G. Seco-Granados, and A. Vazquez-Castro, "SAT03-3: Joint time slot optimization and fair bandwidth allocation for DVB-RCS systems," in *Proc. Globecom*, Jan. 2007, pp. 1–5.
- [37] *Digital Video Broadcasting (DVB): Second Generation DVB Interactive Satellite System (DVB-RCS2): Part 1: Overview and System Level Specification*, document TS 101 545-1 V1.2.1, ETSI, 2014.
- [38] *Digital Video Broadcasting (DVB): Second Generation DVB Interactive Satellite System (DVB-RCS2): Part 3: Higher Layers Satellite Specification*, document TS 101 545-3 V1.2.1, ETSI, 2014.



RENATO F. IIDA received the B.Eng. degree in telecommunications engineering and the M.Sc. degree in electrical engineering from the University of Brasília, Brazil, in 2002 and 2006, respectively. He is currently pursuing the Ph.D. degree in electrical engineering with the Worcester Polytechnic Institute, Worcester, MA, USA. From 2008 to 2014, he worked in system level simulations with Nokia, and was involved in the standardization of MUROS, VAMOS feature in GSM network in 3GPP. He is currently working at Ancud IT. His current research interests include V2V networks and to improve the radio resource management in the type of networks. He received the award from CAPES with science without borders program to support his Ph.D. degree.



PEDRO H. A. TRINDADE received the B.Eng. degree in electronics engineering from the University of Brasília, DF, Brazil, in 2019, where he is currently pursuing the M.Sc. degree in electrical engineering and the B.Sc. degree in mathematics. From 2018 to 2019, he worked in system level simulations and FPGA development for DVB-S2X/DVB-RCS2 satellite networks. His current research interests include optimal resources allocation in satellite communications and game theory.



BRUNO FARIA is currently a Passionate Telecommunications Engineer with great experience on research and development for innovative wireless communication solutions development. As a Multidisciplinary Engineer, he has worked from IP mobility protocol specification within IETF to physical layer analysis and design for future radio access technologies. He has solid experience with modeling, designing, and analyzing wireless communication systems. Currently, he is the Co-Founder and the Lead Telecommunication Engineer at Ektrum, developing research and solutions for the mobile, logistics, and mining industry.



LEONARDO AGUAYO received the B.Eng. and M.Sc. degrees from the University of São Paulo, Brazil, and the Ph.D. degree from the Federal University of Ceará, Brazil. Before joining the University of Brasília, in 2005, he held different positions in industry and academy, performing applied research to Ericsson (with GTEL and UFC) and Nokia. He has experience on microwave radio and mobile cellular planning, TTE (Through-the-Earth) systems, system-level simulations of wireless networks, and neural networks. His current research interests include satellite networks and applications of machine learning to wireless communications.



ALEXANDER M. WYGLINSKI (Member, IEEE) received the B.Eng. degree from McGill University, Montreal, Canada, in 1999, the M.Sc.(Eng.) degree from Queen's University, Kingston, Canada, in 2000, and the Ph.D. degree from McGill University, in 2005, all in electrical engineering. He is currently a Professor of electrical and computer engineering at the Worcester Polytechnic Institute (WPI), Worcester, MA, USA, where he has been the Director of the Wireless Innovation Laboratory, since 2007. His current research interests include wireless communications, cognitive radio, machine learning for wireless systems, software defined radio prototyping, connected and autonomous vehicles, and dynamic spectrum sensing, characterization, and access. Additionally, he served as the President for the IEEE Vehicular Technology Society, from 2018 to 2019, and has been a Technical Editor for the *IEEE Communications Magazine*, since 2011.

...